Nonlinear response of Bloch electrons in infinite dimensions

V. Turkowski* and J. K. Freericks†
Department of Physics, Georgetown University, Washington, D.C. 20057, USA
(Received 20 August 2004; revised manuscript received 23 November 2004; published 4 February 2005)

The nonlinear response of noninteracting (Bloch) electrons is examined within a nonequilibrium formalism on the infinite-dimensional hypercubic lattice. We examine the effects of a spatially uniform, but time-varying electric field (ignoring magnetic-field effects). The electronic Green's functions, Wigner density of states, and time-varying current are all determined and analyzed. We study both constant and pulsed electric fields, focusing on the transient response region and on local properties. These noninteracting Green's functions are an important input into nonequilibrium dynamical mean field theory for the nonlinear response of strongly correlated electrons.

DOI: 10.1103/PhysRevB.71.085104 PACS number(s): 71.10.−w, 72.20.Ht, 71.45.Gm

I. INTRODUCTION

The linear-response theory of Kubo[1] and Greenwood[2] is an attractive approach to understand how electrons (in the solid state) interact with external electromagnetic fields. It can be used (in principle) to calculate general linear-response functions in systems that have arbitrarily strong electron correlations. Surprisingly, the linear-response regime for many bulk materials (especially for parabolic band semiconductors[3–7]) and devices, holds for a wide range of electric field strengths.

But there are a multitude of interesting nonlinear effects in electric fields. Most electronic devices have a nonlinear current-voltage relation (transistors, Josephson junctions, etc.) and there is wide interest in nonlinear effects in bulk materials as well (since it is the nonlinearity that often determines the ultimate performance).

Devices are also becoming smaller and smaller. Semiconductor processing line features are well below 100 nm, and there is significant research effort on nanoscale devices. In the latter case, a potential difference of one volt produces an electric field on the order of 10^7 V/cm for nanometer scaled devices. These fields are large enough for nonlinear effects to be important, if not critical, to determine the proper behavior in an external field. There also has been significant research performed on high energy density pulsed laser experiments, where fields as high as 10^{10} V/cm can easily be attained over a short time scale. In that case, one drives the material out of equilibrium by the pulse, and studies how it relaxes back to an equilibrium distribution (as a means to determine relaxation times, etc.).

There are few theoretical approaches to nonlinear effects in solid-state systems. The formalism was developed independently by Kadanoff and Baym[8] and Keldysh[9,10] in the early 1960s (Baym[11] and Keldysh[12] have each written short historical accounts of their discoveries). These approaches include the effects of external fields to all orders and typically use perturbation theory to determine the effects of many-body interactions.[13] In the 1980s, Wilkins and collaborators[3–7,14–16] spent much effort in developing these ideas further, and in examining nonlinear responses in finite dimensions. Here we extend that work to infinite-dimensional lattices, where we find many of the results for the electronic Green's functions can be determined analytically. Our formalism allows for an analysis of steady-state effects (like the Wannier-Stark ladders[17]) and of transient effects (like the response to a pulsed field). Our focus on the infinite-dimensional problem represents the natural evolution of dynamical mean field theory (DMFT) from equilibrium to nonequilibrium problems. DMFT was introduced fifteen years ago to provide an alternative limit (that of infinite dimensions) where the many body problem could be solved.[18] It has had tremendous success with strongly correlated models like the Falicov-Kimball model,[19–21] the Hubbard model,[22–24] the periodic Anderson model,[25,26] the Holstein model,[27,28] and others being solved in equilibrium (for reviews, see Refs. 29 and 30). The key element of the DMFT is that the self-energy for the lattice problem is local, so the lattice problem can be mapped onto an effective impurity problem in a nonzero time-dependent field. Because these impurity problems can be solved with sophisticated numerical algorithms, these many-body problems can also be solved. After the success seen in model system calculations, many in the field have moved into real materials problems by combining density functional theory with DMFT. The results have been extraordinary for a variety of correlated materials like plutonium,[31,32] vanadium oxide,[33] and transition-metal ferromagnets[34] (see Ref. 35 for a pedagogical review). These results, and many others, show that the DMFT is an accurate and controlled approximation in three dimensions that captures most of the strong-correlation physics in these systems.

The time is now ripe to explore nonequilibrium problems with DMFT. Since the nonequilibrium system on an infinite-dimensional lattice also has a local self-energy, it too can be mapped onto an effective impurity problem, now in a nonvanishing two-time field. In particular, for the Falicov-Kimball model, the action is quadratic in the Fermionic variables, so the Feynman path integral can be evaluated explicitly as the determinant of a continuous matrix operator (even in the presence of the nonvanishing time-dependent field). There are many numerical issues associated with solving the resulting equations, but they appear to be controllable. Here we focus on the noninteracting problem for three

 ©2005 The American Physical Society

main reasons: (i) the noninteracting solution provides an important benchmark in the limit where the interactions vanish; (ii) the calculation of the determinant of a continuous matrix operator requires that operator to be discretized onto a finite grid, with finite time cutoffs on the Kadanoff-Baym contour,[8] so it is important to understand the transient evolution of nonequilibrium solutions (which are simplest to examine for the noninteracting case); and (iii) the generalization of the Hilbert transform from the equilibrium to the nonequilibrium problem is identical to the one used in the noninteracting case, since the self-energy is local. Hence the noninteracting solutions and the formalism used to derive them will have many useful applications to the solution of the strongly correlated nonequilibrium problem. We will present results for that work in a separate publication.

The organization of this contribution is as follows: in Sec. II, we present the formalism for the nonlinear response, in Sec. III, we present our numerical results, and in Sec. IV, we present our conclusions.

II. GREEN'S FUNCTIONS FOR BLOCH ELECTRONS IN AN EXTERNAL ELECTRIC FIELD

The Hamiltonian for tight-binding electrons hopping on a hypercubic lattice (in the absence of any external fields) is

$$\mathcal{H} = -\sum_{ij} t_{ij} c_i^\dagger c_j - \mu \sum_i c_i^\dagger c_i, \tag{1}$$

where t_{ij} is the Hermitian hopping matrix (chosen to be[18] $t_{ij}=t^*/2\sqrt{d}$ for nearest neighbors as $d\to\infty$), and μ is the chemical potential. We shall consider the case when this system is coupled to an external electromagnetic field. An electromagnetic field is described by a scalar potential $\phi(\mathbf{r},t)$ and a vector potential $\mathbf{A}(\mathbf{r},t)$ via

$$\mathbf{E}(\mathbf{r},t) = -\nabla\phi(\mathbf{r},t) - \frac{1}{c}\frac{\partial \mathbf{A}(\mathbf{r},t)}{\partial t} \tag{2}$$

for the electric field, with c the speed of light. We will use the Landau gauge where $\phi=0$ to perform our calculations, so the electric field is described solely by the vector potential. This provides a significant simplification of the formalism for spatially uniform (but possibly time-varying) electric fields.

Unlike many time-dependent Hamiltonians, the effect of the vector potential is not easily described by adding a time-dependent piece to the Hamiltonian in addition to the time-independent piece in Eq. (1). Instead, one uses the so-called Peierls' substitution[15] for the hopping matrix:

$$t_{ij} \to t_{ij} \exp\left[-\frac{ie}{\hbar c}\int_{\mathbf{R}_i}^{\mathbf{R}_j} \mathbf{A}(\mathbf{r},t)\cdot d\mathbf{r}\right], \tag{3}$$

where $\mathbf{R}_i$ is the spatial lattice vector associated with lattice site i (and similarly for site j) and e is the electric charge. Note that the Peierls' substitution is a simplified semiclassical treatment of the electromagnetic field (our vector potential is a classical, not quantum field) and we are ignoring dipole (and multipole) transitions between bands because we consider just a single-band model. In this case, the Hamiltonian of the noninteracting electrons coupled to an electromagnetic field becomes

$$\mathcal{H}(t) = \sum_{ij} t_{ij} \exp\left[-\frac{ie}{\hbar c}\int_{\mathbf{R}_i}^{\mathbf{R}_j} \mathbf{A}(\mathbf{r},t)\cdot d\mathbf{r}\right] c_i^\dagger c_j - \mu\sum_i c_i^\dagger c_i. \tag{4}$$

The corresponding electric field becomes

$$\mathbf{E}(\mathbf{r},t) = -\frac{1}{c}\frac{\partial \mathbf{A}(\mathbf{r},t)}{\partial t}. \tag{5}$$

We will choose the vector potential in such a way that either the field is zero before $t=0$ and is then turned on, or the field becomes asymptotically small as $t\to-\infty$ and it is adiabatically switched on; in this way, the early time Hamiltonian is always given by Eq. (1). We put in by hand the condition of thermal equilibrium (with no electrical current) in the distant past, since a noninteracting system can never establish thermal equilibrium without being in contact with an interacting thermal bath. The magnetic field has a complicated structure in infinite dimensions, because it involves the curl of the vector potential, which would need to be defined correctly for the infinite-dimensional limit. Because we are interested in electric fields with weak spatial dependence, we shall assume the associated magnetic field is small enough that we can neglect it, even though we will allow the electric field to vary in time. This is an approximation, because our electromagnetic fields no longer satisfy Maxwell's equations, unless the field is uniform in space and constant in time. This condition can be relaxed, perhaps by using a gradient expansion for the weak spatial dependence of the fields,[15] but such an approach is cumbersome in infinite dimensions. From now on, we neglect the spatial dependence of the vector potential (i.e., we are considering only spatially uniform but time-varying electric fields).

It is convenient to introduce a momentum-space representation for the Hamiltonian, which becomes

$$\mathcal{H}(t) = \sum_{\mathbf{k}} \left[\epsilon\left(\mathbf{k} - \frac{e\mathbf{A}(t)}{\hbar c}\right) - \mu\right] c_{\mathbf{k}}^\dagger c_{\mathbf{k}}, \tag{6}$$

with $c_{\mathbf{k}}=\Sigma_j c_j \exp[i\mathbf{R}_j\cdot\mathbf{k}]$ and $c_{\mathbf{k}}^\dagger=\Sigma_j c_j^\dagger \exp[-i\mathbf{R}_j\cdot\mathbf{k}]$. Note that the Hamiltonian in Eq. (6) is a special time-dependent Hamiltonian, because it commutes with itself for all times $[\mathcal{H}(t),\mathcal{H}(t')]=0$, which greatly simplifies the analysis of the time-dependent Green's functions developed below.

The expression for the time-ordered single-particle Green's function is defined to be

$$g^T(\mathbf{k},t,t') = -\frac{i}{\hbar}\langle \mathcal{T}(c_{\mathbf{k}}(t)c_{\mathbf{k}}^\dagger(t'))\rangle. \tag{7}$$

Because of the special time dependence of the Hamiltonian, this Green's function can be determined analytically. In Eq. (7), the operators are expressed in a Heisenberg picture, where the time dependence is $O(t)=\exp[it\mathcal{H}(t)]O\times\exp[-it\mathcal{H}(t)]$ with $\mathcal{H}(t)$ determined from Eq. (4), the time ordering symbol $\mathcal{T}$ orders earlier times to the right (with a change of sign when two Fermionic operators are inter-

changed), and the angle brackets indicate a thermal averaging $\langle O\rangle = \mathrm{Tr}[\exp(-\beta\mathcal{H})O]/\mathrm{Tr}[\exp(-\beta\mathcal{H})]$, with $\beta = 1/T$ the inverse temperature and the Hamiltonian being the field free (early-time) Hamiltonian from Eq. (1). We directly solve for the Green's function by finding the time dependence of the momentum-dependent creation and annihilation operators, and then directly solve for the Green's function by taking the relevant expectation values and traces.[15,36,37] The starting point is to calculate the time dependence of the operators:

$$\frac{d}{dt}c_{\mathbf{k}}^{\dagger}(t) = \frac{i}{\hbar}\left[\epsilon\left(\mathbf{k} - \frac{e\mathbf{A}(t)}{\hbar c}\right) - \mu\right]c_{\mathbf{k}}^{\dagger}(t), \tag{8}$$

$$\frac{d}{dt}c_{\mathbf{k}}(t) = -\frac{i}{\hbar}\left[\epsilon\left(\mathbf{k} - \frac{e\mathbf{A}(t)}{\hbar c}\right) - \mu\right]c_{\mathbf{k}}(t), \tag{9}$$

which can be integrated to give

$$c_{\mathbf{k}}^{\dagger}(t) = \exp\left[\frac{i}{\hbar}\int_{-\infty}^{t}\left[\epsilon\left(\mathbf{k} - \frac{e\mathbf{A}(\bar{t})}{\hbar c}\right) - \mu\right]d\bar{t}\right]c_{\mathbf{k}}^{\dagger}, \tag{10}$$

$$c_{\mathbf{k}}(t) = \exp\left[-\frac{i}{\hbar}\int_{-\infty}^{t}\left[\epsilon\left(\mathbf{k} - \frac{e\mathbf{A}(\bar{t})}{\hbar c}\right) - \mu\right]d\bar{t}\right]c_{\mathbf{k}}. \tag{11}$$

It is now easy to find the expression for the time-ordered Green's function by inserting the time dependence from Eqs. (10) and (11) into the definition of the Green's function in Eq. (7) to yield

$$\begin{aligned} g^{T}(\mathbf{k},t,t') = &-\frac{i}{\hbar}\theta(t-t')\exp\left[-\frac{i}{\hbar}\int_{t'}^{t}\left[\epsilon\left(\mathbf{k} - \frac{e\mathbf{A}(\bar{t})}{\hbar c}\right) - \mu\right]d\bar{t}\right] \\ &\times[1 - f(\epsilon(\mathbf{k}) - \mu)] + \frac{i}{\hbar}\theta(t'-t) \\ &\times\exp\left[-\frac{i}{\hbar}\int_{t'}^{t}\left[\epsilon\left(\mathbf{k} - \frac{e\mathbf{A}(\bar{t})}{\hbar c}\right) - \mu\right]d\bar{t}\right] \\ &\times f(\epsilon(\mathbf{k}) - \mu), \end{aligned} \tag{12}$$

since the averages satisfy $\langle c_{\mathbf{k}}^{\dagger}c_{\mathbf{k}}\rangle = f(\epsilon(\mathbf{k}) - \mu)$ and $\langle c_{\mathbf{k}}c_{\mathbf{k}}^{\dagger}\rangle = [1 - f(\epsilon(\mathbf{k}) - \mu)]$ with $f(x) = 1/[1 + \exp(\beta x)]$ being the Fermi-Dirac distribution, and $\epsilon(\mathbf{k})$ the band structure.

In infinite-dimensional calculations, it is important to also determine local properties, like the local Green's function $[g_{loc} = \Sigma_{\mathbf{k}} g(\mathbf{k})]$, the local density of states (DOS), and the local distribution function. Often these local quantities are not examined in nonequilibrium calculations that focus on momentum space in order to make contact with Boltzmann-equation-like approaches (but some previous work has focused on local properties[38]). The Green's function in Eq. (12) depends on both $\epsilon(\mathbf{k})$ and $\epsilon(\mathbf{k} - e\mathbf{A}/\hbar c)$. Hence, the summation over momentum cannot be performed simply by introducing an integral over the noninteracting DOS. Instead, the method of Mueller-Hartmann must be used,[39–41] to perform the integrations over the Brillouin zone and to extract the leading contributions as $d \to \infty$. The algebra is straightforward, but lengthy. The final result is

$$\begin{aligned} g_{loc}^{T}(t,t') = &-\frac{i}{\hbar}\int d\epsilon[\theta(t-t') - f(\epsilon - \mu)] \\ &\times\rho(\epsilon)\exp\left[-i\frac{\epsilon}{\hbar}\frac{1}{d}\sum_{\alpha}\int_{t'}^{t}d\bar{t}\cos\frac{eaA_{\alpha}(\bar{t})}{\hbar c}\right] \\ &\times\exp\frac{t^{*2}}{4\hbar^{2}}\left\{\left[\frac{1}{d}\sum_{\alpha}\int_{t'}^{t}d\bar{t}\cos\frac{eaA_{\alpha}(\bar{t})}{\hbar c}\right]^{2}\right. \\ &\left.-\frac{1}{d}\sum_{\alpha}\int_{t'}^{t}d\bar{t}\int_{t'}^{t}d\bar{t'}\cos\frac{ea\{A_{\alpha}(\bar{t}) - A_{\alpha}(\bar{t'})\}}{\hbar c}\right\} \\ &\times e^{i\mu(t-t')/\hbar}, \end{aligned} \tag{13}$$

where α denotes the component of the vector potential and $\rho(\epsilon) = \exp[-\epsilon^2/t^{*2}]/\sqrt{\pi}t^{*}a^{d}$ is the noninteracting DOS (and a is the lattice spacing). Note that in the limit $\mathbf{A} \to 0$, this reduces to the well-known noninteracting Green's function on a hypercubic lattice.

While the results of Eq. (13) are completely general, they are quite cumbersome for calculations, and it is useful to consider some simpler limits. The easiest case to evaluate, which is what we consider for the remainder of this paper, is to examine the case where the vector potential lies along the (1, 1, 1,…) diagonal $[\mathbf{A}(t) = A(t)(1,1,1,\ldots)]$. This choice simplifies the calculations significantly. In this case, the momentum-dependent Green's function in Eq. (12) depends on just two macroscopic objects—the band structure $\epsilon(\mathbf{k})$ and an additional energy function $\bar{\epsilon}(\mathbf{k}) = -t^{*}\lim_{d\to\infty}\Sigma_{\alpha}\sin(k_{\alpha}a)/\sqrt{d}$:

$$\begin{aligned} g^{T}(\epsilon,\bar{\epsilon},t,t') = \exp&\left[-\frac{i}{\hbar}\int_{t'}^{t}\left\{\epsilon(\mathbf{k})\cos\frac{eaA(\bar{t})}{\hbar c}\right.\right. \\ &\left.\left.+\bar{\epsilon}(\mathbf{k})\sin\frac{eaA(\bar{t})}{\hbar c}\right\}d\bar{t}\right]e^{i\mu(t-t')/\hbar} \\ &\times\left(-\frac{i}{\hbar}\right)[\theta(t-t') - f(\epsilon - \mu)]. \end{aligned} \tag{14}$$

Hence the local Green's function can be found by integrating over a joint density of states[37]

$$\rho_2(\epsilon,\bar{\epsilon}) = \sum_{k}\delta[\epsilon - \epsilon(\mathbf{k})]\delta[\bar{\epsilon} - \bar{\epsilon}(\mathbf{k})], \tag{15}$$

which yields

$$g_{loc}^{T}(t,t') = \int d\epsilon\int d\bar{\epsilon}\rho_2(\epsilon,\bar{\epsilon})g^{T}(\epsilon,\bar{\epsilon},t,t'). \tag{16}$$

Using the techniques of Mueller-Hartman[39–41] again gives the following expression for the joint density of states:

$$\rho_2(\epsilon,\bar{\epsilon}) = \frac{1}{\pi t^{*2} a^d} \exp\left(- \frac{\epsilon^2}{t^{*2}} - \frac{\bar{\epsilon}^2}{t^{*2}} \right). \tag{17}$$

Substituting the joint density of states of Eq. (17) into Eq. (16) and integrating over $\bar{\epsilon}$ gives the final expression for the local Green's function:

$$\begin{aligned} g^T_{loc}(t,t') = & - \frac{i}{\hbar} \int d\epsilon [\theta(t-t') - f(\epsilon-\mu)] \\ & \times \rho(\epsilon) \exp\left[- i \frac{\epsilon}{\hbar} \int_{t'}^{t} d\bar{t} \cos \frac{eaA(\bar{t})}{\hbar c} \right] \\ & \times \exp\left[- t^{*2} \left(\int_{t'}^{t} d\bar{t} \sin \frac{eaA(\bar{t})}{\hbar c} \right)^2 \Big/ 4\hbar^2 \right] \\ & \times e^{i\mu(t-t')/\hbar}. \end{aligned} \tag{18}$$

Of course, the result in Eq. (18) agrees with that of Eq. (13) when the vector potential lies along the diagonal.

III. NUMERICAL RESULTS

A. Current density and Bloch oscillations

We begin by studying the current density of the system in the presence of the electric field. The current operator is determined by the commutator of the polarization operator (defined by $\Pi = \Sigma_i \mathbf{R}_i c_i^\dagger c_i$) with the Hamiltonian of the system. The expression for the α-component of the current-density operator has the following form:

$$\mathbf{j}_\alpha = \frac{eat^*}{\hbar\sqrt{d}} \sum_{\mathbf{k}} \sin\left(\mathbf{k}_\alpha a - \frac{ea\mathbf{A}_\alpha(t)}{\hbar c} \right) c^\dagger_{\mathbf{k}} c_{\mathbf{k}}. \tag{19}$$

The expectation value of the αth component of the current can be easily calculated from the time-ordered Green's function in Eq. (12) in the limit $t' \to t^+$:

$$\begin{aligned} \langle \mathbf{j}_\alpha \rangle &= - i \frac{eat^*}{\sqrt{d}} \sum_{\mathbf{k}} \sin\left(k_\alpha a - \frac{eaA_\alpha(t)}{\hbar c} \right) g^T(\mathbf{k},t,t^+), \\ &= - \frac{eat^{*2}}{4d\pi\hbar} \sin\left(\frac{eaA_\alpha(t)}{\hbar c} \right) \int d\epsilon \frac{df(\epsilon-\mu)}{d\epsilon} \rho(\epsilon), \end{aligned} \tag{20}$$

where the summation over momentum is performed the same way as before. The total magnitude of the current density is just $\sqrt{d}$ times this result, since each component along the diagonal is the same. In the limit of low temperature, we perform a Sommerfeld expansion, which gives

$$\langle j(t) \rangle = \frac{eat^{*2}\rho(\mu)}{4\sqrt{d}\pi\hbar} \sin\left(\frac{eaA(t)}{\hbar c} \right) \tag{21}$$

[with $A(t)$ the value of the vector potential for each component]. Note that in the case of a constant field, $A(t) = -Ect\theta(t)$ is a linear function of t, and the current is sinusoidal, even though the field is time-independent. This is the well-known Bloch oscillation,[42] with a frequency $\omega_{Bloch} = eaE/\hbar$. Since we have no scattering, the system is a perfect conductor, but the periodicity of the lattice restricts the wave vector to lie in the first Brillouin zone which causes the oscillatory current.

One can investigate a current-current correlation function to determine a noise spectrum, but because the current is periodic, the noise profile would be just two delta functions for a constant field, and we will not learn anything interesting from examining the noise.

It is interesting to note that the current is nonzero for the case $A(t) = \text{const}$, which corresponds to the case of zero electric field. This is a consequence of the fact that the vector potential results in a shifting of the Fermi surface. In the case of an interacting system this current will be destroyed by interparticle scattering. In our case, a free-energy analysis will show that the lowest-energy state is the one without any current. There are a number of analogies of the response of this system to the response of a superconductor (such as an ac response to a dc field, the presence of current-carrying states that do not disappear over time, etc.). All of these results are artifacts of the lack of scattering in the system.

To find the resistivity of the system, we consider the case of a uniform static electric field (along the diagonal) of magnitude $E\sqrt{d}$, which is turned on at $t=0$, so that $\mathbf{A}(t) = -\mathbf{E}ct\theta(t)$ [$A_\alpha(t) = -Ect\theta(t)$], and the potential along a path $b(1,1,1,\ldots)/\sqrt{d}$ is equal to $V = -Eb\sqrt{d}$ (the length b is the distance over which we have a potential drop). The expression for the Ohm's law in the form $V = jRa^{d-1}$ (current density multiplied by the resistance-area product), gives the following expression for resistance-area product:

$$Ra^{d-1} = \frac{V}{j} = \frac{4\pi\hbar Edb}{eat^{*2}\rho(\mu)} \Big/ \sin\left(\frac{eaEt}{\hbar} \right). \tag{22}$$

The resistivity is defined to be $1/b$ times the resistance-area product, in the linear-response limit of $E \to 0$. Therefore,

$$\rho_{lin.\ resp.} = \frac{4\pi\hbar^2 d}{e^2 a^2 t^{*2} \rho(\mu)} \frac{1}{t}. \tag{23}$$

This result is proportional to d, as it should be because the conductivity is proportional to $1/d$ in infinite dimensions. The correct resistivity is zero for a noninteracting system. Here we see that the linear-response resistivity in Eq. (23) goes to zero in the limit of large time $t \to \infty$.

Let us estimate the linear response resistance of the ballistic metal from the expression in Eq. (23), which can be finite because the linear-response resistance has a factor of b/t in it. For the ballistic metal the length b over which the electrons have moved in the time t should be $b = v_F t$, with v_F a suitable average of the Fermi velocity. This gives the resistance

$$R_{lin.\ resp.} = \frac{4\pi\hbar^2 v_F d}{e^2 a^{d+1} t^{*2} \rho(\mu)}. \tag{24}$$

This expression corresponds to the Sharvin resistance[43,44] for a single-band model in infinite dimensions. In three dimensions, the Sharvin resistance is $h/2e^2$ divided by the number of channels, which is a Fermi surface factor multiplied by $4\pi/k_F^2 Area$. To compare with our formula, we must first note that we map the hopping integral onto the effective mass (for low electron filling) via

$$t^* = \frac{\hbar^2\sqrt{d}}{ma^2} \tag{25}$$

and that $a^d t^* \rho(\mu) = C$ is a constant of order one [proportional to $(k_F a)^{d-2}$ for low filling]. Therefore,

$$R_{lin.\ resp.} = \frac{4\pi m v_F a\sqrt{d}}{e^2 C} \propto \frac{h}{2e^2}\frac{4\sqrt{d}}{(k_F a)^{d-3}}, \tag{26}$$

which has a Sharvin-like form (but appears to have the wrong dependence on $k_F a$ for $d=3$; this most likely is an artifact of the problems with assuming a spherical Fermi surface in large dimensions, which is valid only for vanishing electron densities).

We can also investigate the heat current carried when there is an electrical field present (but no temperature gradient), and we find that its average value vanishes at half filling, as expected, because the thermopower vanishes at half filling, and we have no thermal gradients to directly drive a thermal current (in the general case, the energy part of the current vanishes, and the chemical potential piece will give a contribution of $-\mu\mathbf{j}$ to the heat current). So heat transport is trivial unless one introduces a thermal gradient to the temperature, which we do not do here.

B. Local density of states

Next we examine the spectral function and the density of states in the presence of a field. The time-dependent spectral function can be calculated from the retarded Green's function $g^R(t,t') = -(i/\hbar)\theta(t-t')\langle\{c(t), c^\dagger(t')\}\rangle$ (with the operators expressed in a Heisenberg picture) using the Wigner coordinates[45] by introducing the average time $t_{ave} = (t+t')/2$ and the relative time $t_{rel} = t - t'$ variables. In this case, the spectral function as a function of the average time (and Fourier transformed over the relative time) is equal to

$$A(t_{ave}, \mathbf{k}, \omega) = -\frac{1}{\pi}\,\mathrm{Im}\int_0^\infty dt_{rel} e^{i\omega t_{rel}} g^R(\mathbf{k}, t_{ave}, t_{rel}), \tag{27}$$

and the DOS is equal to

$$A(t_{ave}, \omega) = -\frac{1}{\pi}\,\mathrm{Im}\int_0^\infty dt_{rel} e^{i\omega t_{rel}} g^R_{loc}(t_{ave}, t_{rel}). \tag{28}$$

In general, the retarded Green's function can be found from the same technique used to calculate the time-ordered Green's function: first one introduces the time dependence of the Heisenberg operators, then one evaluates the operator averages. Since the anticommutator of two local creation and annihilation operators (or two operators in the momentum basis) is equal to one, we get

$$g^R(\mathbf{k}, t, t') = -\frac{i}{\hbar}\theta(t-t')e^{i\mu(t-t')/\hbar} \times \exp\left[-i\frac{\epsilon(\mathbf{k})}{\hbar}\int_{t'}^{t} d\bar{t}\cos\frac{eaA(\bar{t})}{\hbar c}\right] \times \exp\left[-i\frac{\bar{\epsilon}(\mathbf{k})}{\hbar}\int_{t'}^{t} d\bar{t}\sin\frac{eaA(\bar{t})}{\hbar c}\right] \tag{29}$$

for the momentum-dependent Green's function and

$$g^R_{loc}(t,t') = -\frac{i}{\hbar}\theta(t-t')\int d\epsilon\rho(\epsilon)e^{i\mu(t-t')/\hbar} \times \exp\left[-i\frac{\epsilon}{\hbar}\int_{t'}^{t} d\bar{t}\cos\frac{eaA(\bar{t})}{\hbar c}\right] \times \exp\left[-t^{*2}\left(\int_{t'}^{t} d\bar{t}\sin\frac{eaA(\bar{t})}{\hbar c}\right)^2 \Big/ 4\hbar^2\right], \tag{30}$$

for the local Green's function (using the t and t' coordinates). Note that these Green's functions have no temperature dependence, hence the spectral function and the DOS are independent of temperature. This is characteristic of a noninteracting system.

The spectral function, in the absence of a field, is a delta function $[A(\mathbf{k},\omega) = \delta(\omega - \epsilon(\mathbf{k}) + \mu)]$. When a field is turned on, the time dependence is no longer a pure exponential, so the spectral function deviates from the delta function, becoming a peaked function of nonvanishing width. In the limit where $t_{ave} \to \infty$, the steady state is approached and the spectral function becomes a set of evenly spaced delta functions, since the Green's function becomes a periodic function in t_{rel}.

The analysis for the local DOS is more complicated. Since the ϵ dependence in Eq. (30) is so simple, the integral can be performed directly, with the result

$$g^R_{loc}(t_{ave}, t_{rel}) = -\frac{i}{\hbar}\theta(t_{rel})e^{i\mu t_{rel}/\hbar}\exp\left[-\frac{t^{*2}}{4\hbar^2}|I(t_{ave}, t_{rel})|^2\right], \tag{31}$$

where

$$I(t_{ave}, t_{rel}) = \int_{t_{ave}-t_{rel}/2}^{t_{ave}+t_{rel}/2} d\bar{t}\exp\left[i\frac{eaA(\bar{t})}{\hbar c}\right]. \tag{32}$$

In order to evaluate some numerical results, we first consider the case of a constant electric field turned on at $t=0$. In this case, we get

$$I(t_{ave},t_{rel}) = \theta(-t_{ave}-t_{rel}/2)\,\theta(-t_{ave}+t_{rel}/2)t_{rel} + \theta(-t_{ave}-t_{rel}/2)\,\theta(t_{ave}-t_{rel}/2)\left[t_{ave}+t_{rel}/2+(1-e^{i(eaE/\hbar)(t_{ave}-t_{rel}/2)})\frac{\hbar}{ieaE}\right]$$
$$+\,\theta(t_{ave}+t_{rel}/2)\,\theta(-t_{ave}+t_{rel}/2)\left[(e^{i(eaE/\hbar)(t_{ave}+t_{rel}/2)}-1)\frac{\hbar}{ieaE}-t_{ave}+t_{rel}/2\right]+\theta(t_{ave}+t_{rel}/2)\,\theta(t_{ave}-t_{rel}/2)$$
$$\times\frac{\hbar}{ieaE}(e^{i(eaE/\hbar)(t_{ave}+t_{rel}/2)}-e^{i(eaE/\hbar)(t_{ave}-t_{rel}/2)}). \tag{33}$$

This result has some interesting properties. If $E\to 0$, then $I=t_{rel}$ for all t_{ave}, and g^R_{loc} is a Gaussian in t_{rel}, which Fourier transforms to a Gaussian in frequency, i.e., it becomes the noninteracting DOS. There is an interesting scaling behavior. If we define $\overline{t_{ave}}=t_{ave}eaE/\hbar$, $\overline{t_{rel}}=t_{rel}eaE/\hbar$, and $\overline{\omega}=\omega\hbar/eaE$, then

$$I(t_{ave},t_{rel}) = \frac{\hbar}{eaE}\overline{I}(\overline{t_{ave}},\overline{t_{rel}}), \tag{34}$$

with $\overline{I}$ a function independent of E. Hence

$$g^R_{loc}(\overline{t_{ave}},\overline{t_{rel}}) = -\frac{i}{\hbar}\theta(\overline{t_{rel}})e^{i\mu\overline{t_{rel}}/eaE}$$
$$\times\exp\left[-\frac{t^{*2}}{4e^2a^2E^2}|\overline{I}(\overline{t_{ave}},\overline{t_{rel}})|^2\right], \tag{35}$$

and the DOS becomes

$$A(\overline{t_{ave}},\overline{\omega}) = -\frac{1}{\pi}\,\mathrm{Im}\int_0^\infty d\overline{t_{rel}}e^{i\overline{\omega}\overline{t_{rel}}}g^R_{loc}(\overline{t_{ave}},\overline{t_{rel}}), \tag{36}$$

with the normalization chosen so $\int d\overline{\omega}A(\overline{\omega})=1$ (for easier comparison of curves for different E). Hence we expect the DOS to have the same shape as a function of $\overline{\omega}$ (with a possible shift due to the chemical potential factor), but the amplitude of the oscillations grows as E increases [because of the minus sign in the exponent in Eq. (35)]. But that turns out only to be true near $\omega=0$. At other frequencies, the evolution with E is not always monotonic, because the DOS conserves total spectral weight, so there cannot be a monotonic evolution of the peaks at all frequencies.

Note that the DOS satisfies two properties in equilibrium. The first is that the integral over frequency equals 1. The second is that the DOS is always positive. The proof for the integral yielding 1 holds even in the nonequilibrium case, because the anticommutator of two Fermionic creation and annihilation operators at the same time is still one. The positivity does not hold, because the standard derivation, using the spectral representation, requires the Hamiltonian to be independent of time in order to be able to be used, and thereby prove the positivity. Indeed, the DOS in the presence of a field has regions where it is negative.

It is interesting to consider the limit of large t_{ave}, i.e., $t_{ave}\to\infty$, then we get the steady-state solution. We take only the last term of $I(t_{ave},t_{rel})$ in Eq. (33) because t_{ave} is always larger than t_{rel} in this limit. The Green's function becomes

$$g^R_{loc}(t_{ave}\to\infty,t_{rel}) = -\frac{i}{\hbar}\theta(t_{rel})$$
$$\times\exp\left[\frac{t^{*2}}{2e^2a^2E^2}\left(\cos\left(\frac{eaE}{\hbar}t_{rel}\right)-1\right)\right]. \tag{37}$$

The Fourier transform of this is a set of delta functions, with different amplitudes, that are equally spaced in frequency, with a spacing $eaE/\hbar$ (since the Green's function is periodic in t_{rel}). This is the famous Wannier-Stark ladder,[17] expected for systems placed in an external electric field. In the results plotted in Fig. 1, the fact that the peaks at multiples of this frequency get larger, and grow in height as t_{ave} grows, indicates our results are showing the correct buildup to the steady state, but they will never get there until $t_{ave}\to\infty$. It is no coincidence that this frequency is the same as the Bloch oscillation frequency. This discussion was first described in detail from the Green's function approach by Davies and Wilkins.[16] Note that the DOS is non-negative in the steady state.

We can calculate the weight of the delta functions by performing the Fourier series integral. The frequencies are $NeaE/\hbar$, and the Fourier coefficient is

$$w_N = \frac{2}{eaE}\int_0^{2\pi\hbar/eaE} dt_{rel}\cos\left(\frac{NeaE}{\hbar}t_{rel}\right)$$
$$\times\exp\left[\frac{t^{*2}}{2e^2a^2E^2}\left(\cos\left(\frac{eaE}{\hbar}t_{rel}\right)-1\right)\right]$$
$$=\frac{2\hbar}{e^2a^2E^2}\int_0^{2\pi} du\cos(Nu)\exp\left(\frac{t^{*2}}{2e^2a^2E^2}[\cos u-1]\right). \tag{38}$$

For our numerical results, we examine how the system approaches the steady state as the field is turned on. We work at half filling ($\mu=0$), where the DOS is symmetric; hence, we plot only the results for positive frequencies. The field needs to be large enough for our calculations to be able to see the nonlinear effects of the field on the DOS. For us, the numerical results can easily see effects on the DOS when $eaE/\hbar>0.1$. In Fig. 1, we plot results for $eaE/\hbar=1$. While it is true that the Green's functions for t and t' both less than zero are equal to their equilibrium (field-free) limit, the Wigner DOS feels the effect of the fields for all finite t_{ave}, because the integral over t_{rel} always includes some Green's

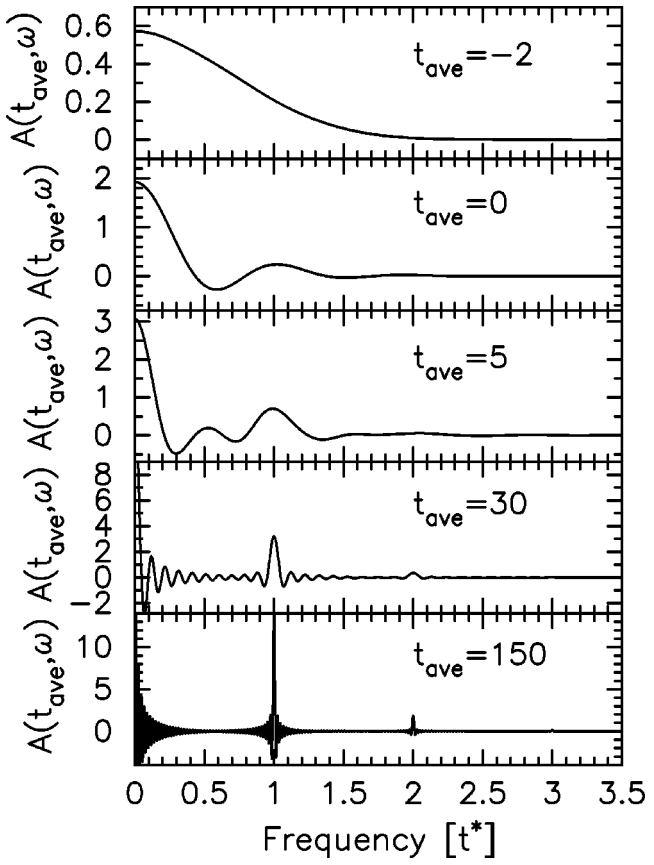

FIG. 1. Density of states $A(t_{ave},\omega)$ (in units $1/a^d t^*$ with a the lattice spacing and $d\to\infty$ the spatial dimension) for noninteracting electrons with $eaE/\hbar=1$. Note how the DOS is essentially a Gaussian for $t_{ave}<-2$, but then develops large oscillations as t_{ave} increases. The DOS approaches a steady state for large time given by a set of delta functions, equally spaced by the Bloch oscillation frequency. The DOS is no longer positive once the field is turned on, but the integral does always equal 1.

functions with either t or t' larger than zero. We can see that significant "precursor" effects occur only for $t_{ave}>-2$ here, and the DOS develops significant oscillations before one can see the delta functions start to build up at the integer frequencies.

We plot a close up of the region around $\omega=1$ in Fig. 2. Note how a sharp peak develops as the average time increases, but there are significant oscillations near $\omega=1$ whose amplitude decreases slowly as t_{ave} increases.

In Fig. 3, we plot the DOS in the $\bar{\omega}$ variable near $\bar{\omega}=0$ for $\bar{t}_{ave}=100$ and for five values of $eaE/\hbar$ (0.1, 0.3, 1.0, 3.0, and 10.0). This shows how the oscillations grow as E increases. For other integer values of ω, the evolution is not monotonic in the field strength E (for example, at $\omega=1$ the peak values increase with E for $0.1<eaE/\hbar<0.7$ and then decrease for $0.7<eaE/\hbar<10$).

C. Distribution functions

In addition to the spectral function and the DOS, it is interesting to examine the distribution function. In equilibrium, the distribution function is a Fermi-Dirac distribution

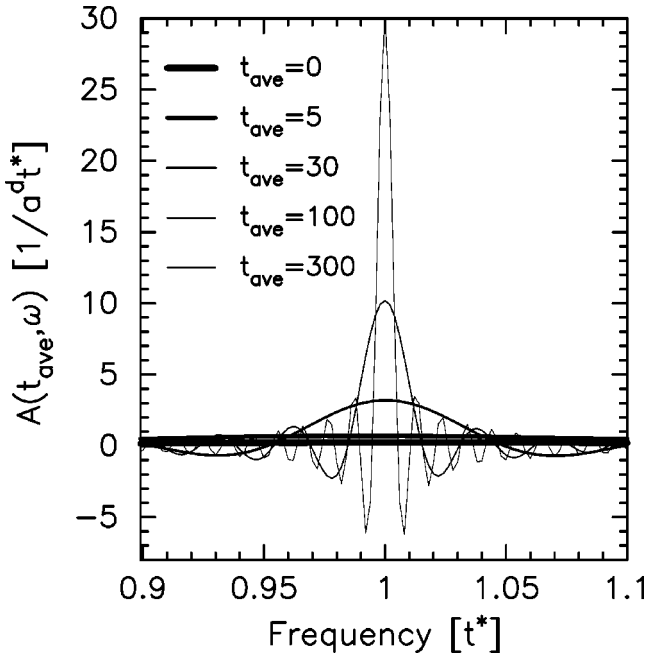

FIG. 2. Close up of the density of states $A(t_{ave},\omega)$ near $\omega=1$ for noninteracting electrons with $eaE/\hbar=1$. Note how the DOS approaches a steady state for large time by developing a sharp peak, but that there are significant oscillations near the sharp peak that decay slowly in time.

function, but the distribution function can change for nonequilibrium cases. In order to discuss distribution functions, we need to define two more Green's functions—the so-called lesser and greater Green's functions. They are defined as $g^{>}(t,t')=-(i/\hbar)\langle c(t)c^{\dagger}(t')\rangle$ and $g^{<}(t,t')=(i/\hbar)\langle c^{\dagger}(t')c(t)\rangle$

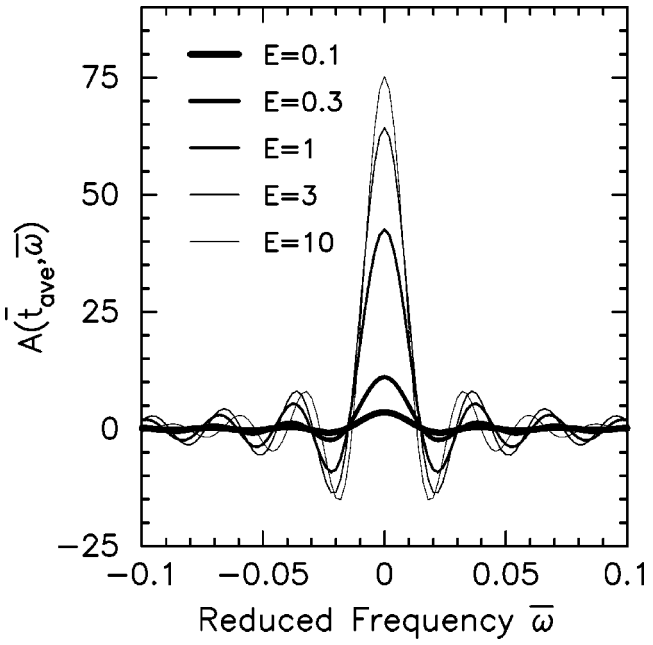

FIG. 3. Close up of the dimensionless density of states $A(\bar{t}_{ave},\bar{\omega})$ near $\bar{\omega}=0$ for noninteracting electrons with $eaE/\hbar=0.1$, 0.3, 1.0, 3.0, and 10.0. Note how the peak in the DOS evolves as a function of the electric field.

(with the operators expressed in a Heisenberg picture). These Green's functions can also be determined for Bloch electrons, and their expressions are the same as those for the retarded Green's function in Eqs. (29) and (30), except the $\theta(t-t')$ factor is replaced by $-f(\epsilon(\mathbf{k})-\mu)$ for $g^<$ and by $[1-f(\epsilon(\mathbf{k})-\mu)]$ for $g^>$. There are three cases for the distribution function that we can consider (the Wigner distribution, the quasiparticle distribution, and the local quasiparticle distribution). The most often used distribution function is the Wigner distribution function, defined to be

$$f_{Wigner}(t_{ave},\mathbf{k}) = -i\hbar g^<(\mathbf{k}, t=t_{ave}, t'=t_{ave}). \tag{39}$$

The Wigner distribution function is always equal to the field-free Fermi-Dirac result $f_{Wigner}(t_{ave},\mathbf{k})=f(\epsilon(\mathbf{k})-\mu)$ for Bloch electrons. The quasiparticle distribution function is defined in analogy with the equilibrium result $[g^<(\mathbf{k},\omega) = 2\pi i f(\omega)A(\mathbf{k},\omega)]$ via

$$f_{quasi}(t_{ave},\mathbf{k}) = \frac{1}{2\pi}\frac{\mathrm{Im}\, g^<(t_{ave},\mathbf{k},\omega)}{A(t_{ave},\mathbf{k},\omega)} \tag{40}$$

(note that the name quasiparticle distribution does not necessarily imply that there must be an underlying Fermi liquid in the system). Since the only difference between the retarded Green's function and the lesser Green's function is the replacement of the theta function by the Fermi-Dirac distribution (which does not depend on the time variables), the ratio of the two terms in Eq. (40) has an explicit factor of $f(\epsilon(\mathbf{k})-\mu)$. The Fourier transform of the numerator is over all t_{rel}, while the denominator is only over all positive t_{rel}. The integral $I(t_{ave},t_{rel})$ is an odd function of t_{rel} [see Eq. (32)], which implies the numerator in Eq. (40) is $2\pi f(\epsilon(\mathbf{k})-\mu)A(t_{ave},\mathbf{k},\omega)$, and we find the quasiparticle distribution function is equal to the Fermi-Dirac distribution once again. The final distribution function to be defined is the local quasiparticle distribution function. This is

$$f^{loc}_{quasi}(t_{ave}) = \frac{1}{2\pi}\frac{\mathrm{Im}\, g^<_{loc}(t_{ave},\omega)}{A(t_{ave},\omega)}. \tag{41}$$

This distribution function is nontrivial in a field, because the DOS and the lesser Green's function both have oscillations, but the zeros occur at different locations on the frequency axis, so the ratio in Eq. (41) can have significant oscillations.

The calculation of the local quasiparticle distribution function is difficult because the presence of an $f(\epsilon-\mu)$ factor precludes us from performing the integral over ϵ analytically; hence the numerical computations are more involved. We need to evaluate the integral

$$g^<(t_{ave},t_{rel}) = \frac{i}{\hbar}\int d\epsilon\rho(\epsilon)f(\epsilon-\mu) \times\exp\left[-i\frac{\epsilon}{\hbar}x(t_{ave},t_{rel}) - \frac{t^{*2}}{4\hbar^2}y^2(t_{ave},t_{rel})\right] \tag{42}$$

numerically, with $x=\mathrm{Re}\, I$, $y=\mathrm{Im}\, I$, and I being the integral in Eq. (32). If $eaE/\hbar=0$, then this is just the Fourier transform of $2\pi i f(\omega)\rho(\omega)$, which gives the correct lesser function. If $eaE/\hbar\neq 0$, then the Green's function has to be calculated numerically. Because the real part of the lesser Green's function is nonzero for a longer range in time than the imaginary part, the function $g^<$ will have more oscillations than the g^R function. The results for a local quasiparticle distribution function are plotted in Fig. 4. As it follows from this figure, the local quasiparticle distribution function varies significantly from the equilibrium values as t_{ave} increases. This is because the $g^<$ Green's function has high frequency oscillations, which are not as strong in the DOS. The oscillations continue as t_{ave} increases, but they become difficult to plot. Of course the momentum-dependent quasiparticle distribution function is equal to the Fermi-Dirac distribution function for this problem.

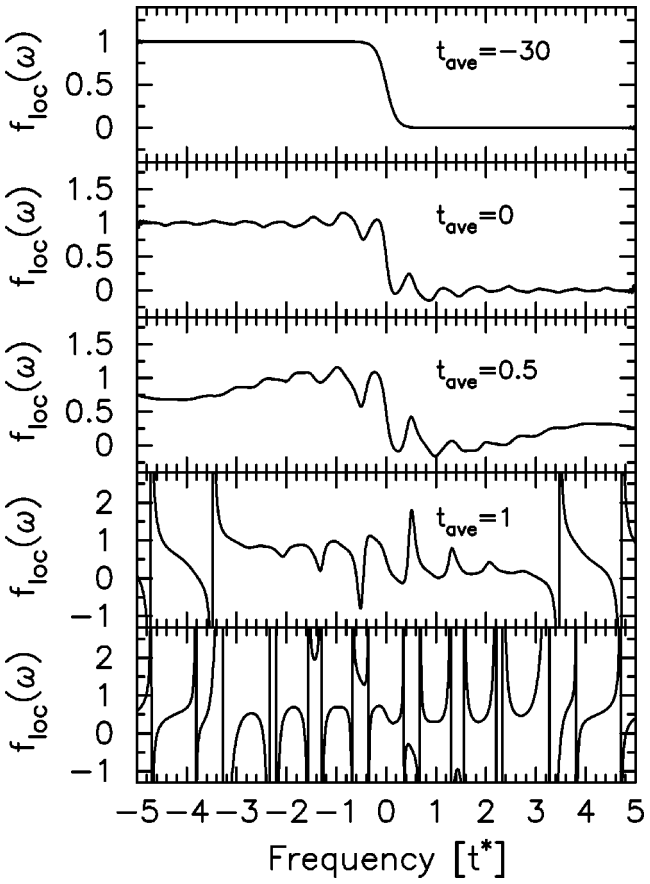

FIG. 4. Local quasiparticle distribution function $f_{loc}(t_{ave},\omega)$ for noninteracting electrons with $eaE/\hbar=1$ and $T=0.1$. Note how the local quasiparticle distribution function varies significantly from the equilibrium values as t_{ave} increases (the lowest panel is for $t_{ave}=2$). This is because the $g^<$ Green's function has high frequency oscillations, which are not as strong in the DOS. The oscillations continue as t_{ave} increases, but they become difficult to plot.

Finally, we study the time dependence of the DOS for the case of a sharp pulse during the period of time $0<t<t_E$. The second derivative of the vector potential is proportional to the strength of the magnetic field (which we are neglecting), so we want to keep the second derivative small for the calculations to make sense. We choose the electric field to have the following time dependence: $E(t)=E\theta(t_E-t)\theta(t)$, which corresponds to a vector potential

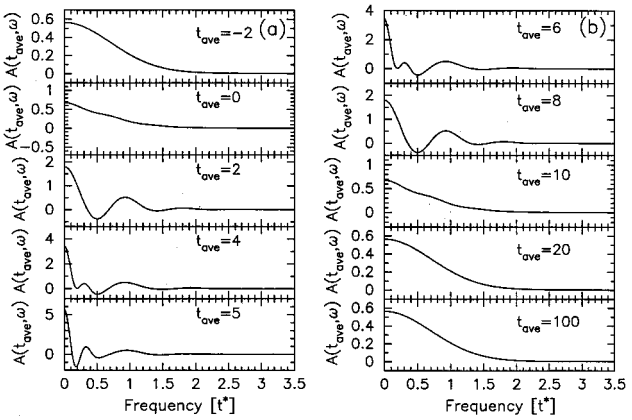

FIG. 5. Local DOS (in units $1/a^d t^*$) for the case of a sharp flat pulse with $eaE/\hbar=1.0$, $t_E=10.0$, and various average times. The horizontal scale is the same in every panel, but the vertical scale changes in the different panels. By comparing figure (a) with figure (b), one can see that the response is identical for times t_{ave} and t'_{ave} that satisfy $t_{ave}+t'_{ave}=t_E$.

$$A(t) = -cEt\theta(t_E - t)\theta(t) - cEt_E\theta(t - t_E). \tag{43}$$

Note that these results are "singular" for the noninteracting case, because the final vector potential is a constant that can correspond to a current carrying state if the Fermi surface is shifted from the zone center. Because there is no scattering, such a current lives forever (but would decay in the presence of any scattering). Numerical calculations show that the DOS deviates visibly from its equilibrium value during the times $|t|<t_{relax}$ when the amplitude of the field is larger or on the order of t^*; the relaxation time t_{relax} is on the order of the pulse time t_E.

The results of the calculations are presented in Fig. 5 for $eaE/\hbar=1$ (when $eaE/\hbar$ is much smaller than 1, the oscillations become hard to see). The nonequilibrium DOS shows oscillating behavior, which then decays as time increases. The results satisfy a symmetry relation, where the Wigner DOS is identical for t_{ave} and t'_{ave} when $t_{ave}+t'_{ave}=t_E$.

We also consider the case of a smooth pulse with a smooth turnon and turnoff of the electric field: $A(t)=Ect_E\exp(-t^2/t_E^2)/2$ [which corresponds to an electric field $E(t)=Et/t_E\exp(-t^2/t_E^2)$]. This field changes sign at $t=0$ and has it maximum amplitude at $t=\pm\sqrt{0.5}$. The Wigner DOS is symmetric in t_{ave}, so we only plot results for positive times in Fig. 6. Note that at $t_{ave}=0$ the field has been on for a long time, so the result is far from a Gaussian. The amplitude of the peak in the DOS at $\omega=0$ is largest at $t_{ave}=\pm\sqrt{0.5}$, and decays rapidly for larger times.

The proof of the symmetry relation for the Wigner DOS is rather straightforward to do. If the vector potential $A(t)$ has definite parity, $A(-t)=\pm A(t)$, then it is easy to see from Eq. (32) that $I(-t_{ave},t_{rel})=I(t_{ave},t_{rel})$ for even functions and $I(-t_{ave},t_{rel})=I(t_{ave},t_{rel})^*$ for odd functions. Since it is the modulus of I that enters into the calculation of $A(t_{ave},\omega)$, the DOS will satisfy the given symmetry rules. For the case of the constant-field pulse, we need to shift the time axis by $t_E/2$ and shift the vector potential by $Et_E/2$ to have a vector potential that is odd in time. The shift of the vector potential has no effect on the modulus of I, since it contributes only a phase, while the shift in the time axis is precisely what is needed to give the symmetry relation described above. For the Gaussian pulse, the vector potential is already an even function, and the symmetry relation follows directly.

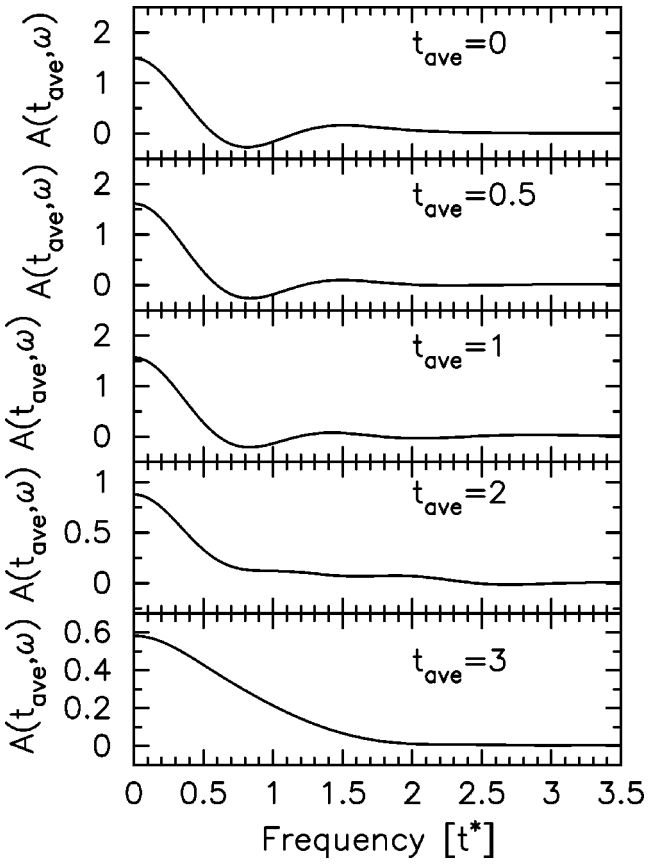

FIG. 6. Local DOS (in units $1/a^d t^*$) for the case of a smooth Gaussian pulse with $eaE/\hbar=10.0$, $t_E=1.0$, and various average times. The results are completely symmetric between negative and positive average times, so we plot only the positive times here. Note how the oscillations are already strong at $t_{ave}=0$, first increase slightly, then fade away as the average time increases.

Note that we do not calculate the experimental probe of the reflectivity as a function of time after the initial pulse, because this system has no intrinsic scattering, so the optical conductivity is always a delta function peak at zero frequency, hence we would not learn anything interesting from such an exercise here. It would be interesting to probe such behavior in systems with intrinsic scattering mechanisms, to understand how the different relaxation mechanisms can be detected.

We end with a discussion about gauge invariance. Our calculations have been performed in a specific gauge (one with the scalar potential vanishing). One can construct retarded Green's functions that are gauge invariant[46] by transforming away the scalar and vector potentials. Since we have spatially uniform fields, the gauge-invariant Green's function is related to our Green's function via the following transformation

$$\tilde{g}^R(\mathbf{k}, t_{ave}, t_{rel}) = g^R\left(\mathbf{k} - \frac{1}{\hbar c t_{rel}} \int_{-t_{rel}/2}^{t_{rel}/2} e\mathbf{A}(t_{ave} + \bar{t})d\bar{t}, t_{ave}, t_{rel}\right), \tag{44}$$

where $\tilde{g}^R$ is the gauge-invariant retarded Green's function. This transformation amounts to a t_{rel}-dependent shift of the momentum wavevector. If we have a constant electric field turned on at $t=0$, and the average time is large, then the shift becomes independent of t_{rel}, so all of our local quantities become gauge invariant when t_{ave} is large enough. In other cases, one has to first shift the momentum, and then Fourier transform the relative time to a frequency, which is quite complicated for the general case.

IV. CONCLUSIONS

We have studied the nonlinear response of Bloch electrons to an external time varying (but spatially homogeneous) electric field by employing a nonequilibrium formalism on an infinite dimensional hypercubic lattice. We found that the current showed Bloch oscillations, even when the electric field was constant in time, and we derived a form for the Sharvin-like resistance of the system.

The time dependence of the DOS was calculated. We showed that it becomes a Wannier-Stark ladder for long times, but the transient evolution toward those discrete delta functions had a complex structure, that survives out to long times. We also examined a number of different kinds of distribution functions, and showed that the most commonly chosen distribution functions retained the Fermi-Dirac form regardless of the strength of the electric field (but the local quasiparticle distribution shows complex oscillatory behavior). For pulsed fields, we saw the transient response build and then decay. The amplitude of the oscillations was proportional to the amplitude of the electric field E for a wide range of field strengths, and we needed the field to be sufficiently large ($eaE/\hbar \sim t^*$) before they could be easily seen. Of course, the oscillations decay at times larger than the pulse time.

Finally, we discuss the relationship of this work to the interacting case of the Falicov-Kimball model (where one can examine nonequilibrium properties of a Mott insulator). In this case, we map the lattice problem onto an effective impurity problem in a time-dependent field that depends independently on two time variables. Working in a real-time representation, the impurity action on the Kadanoff-Baym contour is quadratic in the fermionic variables, and hence is equal to the determinant of a continuous matrix operator. After introducing a discretized version of that operator, the nonequilibrium impurity problem can be solved in exactly the same way as the equilibrium problem, but now in a real-time basis. Finally, the generalization of the Hilbert transform, via the joint DOS in Eq. (17), is employed to complete the DMFT self-consistency loop. We will present details of this algorithm, numerical strategies for solving the self-consistency problem, and numerical results for the nonlinear response of Mott insulators in another publication.

ACKNOWLEDGMENTS

We would like to thank J. Serene and V. Zlatić for useful discussions. We acknowledge support from the National Science Foundation under Grant No. DMR-0210717 and the Office of Naval Research under Grant No. N00014-99-1-0328.

*Electronic address: turk@physics.georgetown.edu; URL: http://www.physics.georgetown.edu/~turk
†Electronic address: freericks@physics.georgetown.edu; URL: http://www.physics.georgetown.edu/~jkf

[1] R. Kubo, J. Phys. Soc. Jpn. **12**, 570 (1957).
[2] D. A. Greenwood, Proc. Phys. Soc. London **71**, 585 (1958).
[3] S. K. Sarker, J. H. Davies, F. S. Khan, and J. W. Wilkins, Phys. Rev. B **33**, 7263 (1986).
[4] F. S. Khan, J. H. Davies, and J. W. Wilkins, Phys. Rev. B **36**, 2578 (1987).
[5] P. Lipavský, F. S. Khan, F. Abdolsalami, and J. W. Wilkins, Phys. Rev. B **43**, 4885 (1991).
[6] P. Lipavský, F. S. Khan, A. Kalvová, and J. W. Wilkins, Phys. Rev. B **43**, 6650 (1991).
[7] P. Lipavský, F. S. Khan, and J. W. Wilkins, Phys. Rev. B **43**, 6665 (1991).
[8] L. P. Kadanoff and G. Baym, *Quantum Statistical Mechanics* (Benjamin, New York, 1962).
[9] L. V. Keldysh, Zh. Eksp. Teor. Fiz. **47**, 1945 (1964).
[10] L. V. Keldysh, Sov. Phys. JETP **20**, 1018 (1965).
[11] G. Baym, *Progress in Nonequilibrium Green's Functions*, edited by M. Bonitz (World Scientific, River Edge, NJ, 2000), p. 17.
[12] L. V. Keldysh, *Progress in Nonequilibrium Green's Functions II*, edited by M. Bonitz and D. Semkat (World Scientific, River Edge, NJ, 2003), p. 4.
[13] J. Rammer and H. Smith, Rev. Mod. Phys. **58**, 323 (1986).
[14] A. P. Jauho and J. W. Wilkins, Phys. Rev. Lett. **49**, 762 (1982).
[15] A. P. Jauho and J. W. Wilkins, Phys. Rev. B **29**, 1919 (1984).
[16] J. H. Davies and J. W. Wilkins, Phys. Rev. B **38**, 1667 (1988).
[17] G. H. Wannier, Rev. Mod. Phys. **34**, 645 (1962).
[18] W. Metzner and D. Vollhardt, Phys. Rev. Lett. **62**, 324 (1989).
[19] U. Brandt and C. Mielsch, Z. Phys. B: Condens. Matter **75**, 365 (1989).
[20] U. Brandt and C. Mielsch, Z. Phys. B: Condens. Matter **79**, 295 (1990).
[21] U. Brandt and C. Mielsch, Z. Phys. B: Condens. Matter **82**, 37 (1991).
[22] M. Jarrell, Phys. Rev. Lett. **69**, 168 (1992).
[23] M. J. Rozenberg, X. Y. Zhang, and G. Kotliar, Phys. Rev. Lett. **69**, 1236 (1992).
[24] R. Bulla, Phys. Rev. Lett. **83**, 136 (1999).
[25] M. Jarrell, H. Akhlaghpour, and T. Pruschke, Phys. Rev. Lett. **70**, 1670 (1993).
[26] T. Pruschke, R. Bulla, and M. Jarrell, Phys. Rev. B **61**, 12 799

(2000).
[27] J. K. Freericks, M. Jarrell, and D. J. Scalapino, Phys. Rev. B **48**, 6302 (1993).
[28] D. Meyer, A. C. Hewson, and R. Bulla, Phys. Rev. Lett. **89**, 196401 (2002).
[29] A. Georges, G. Kotliar, W. Krauth, and M. J. Rozenberg, Rev. Mod. Phys. **68**, 13 (1996).
[30] J. K. Freericks and V. Zlatić, Rev. Mod. Phys. **75**, 1333 (2003).
[31] S. Savrasov, G. Kotliar, and E. Abrahams, Nature (London) **410**, 793 (2001).
[32] X. Dai, S. Y. Savrasov, G. Kotliar, A. Migliori, H. Ledbetter, and E. Abrahams, Science **300**, 953 (2003).
[33] K. Held, G. Keller, V. Eyert, D. Vollhardt, and V. I. Anisimov, Phys. Rev. Lett. **86**, 5345 (2001).
[34] I. Yang, S. Y. Savrasov, and G. Kotliar, Phys. Rev. Lett. **87**, 216405 (2001).
[35] G. Kotliar and D. Vollhardt, Phys. Today **57**, 53 (2004).
[36] P. Schmidt and H. Monien, cond-mat/0202046.
[37] P. Schmidt, Diplome thesis, University of Bonn, 2002.
[38] A. P. Jauho and K. Johnsen, Phys. Rev. Lett. **76**, 4576 (1996).
[39] E. Müller-Hartmann, Z. Phys. B: Condens. Matter **74**, 507 (1989).
[40] E. Müller-Hartmann, Z. Phys. B: Condens. Matter **76**, 211 (1989).
[41] E. Müller-Hartmann, Int. J. Mod. Phys. B **3**, 2169 (1989).
[42] N. W. Ashcroft and N. D. Mermin, *Solid State Physics* (Holt, Rinehart and Winston, Philadelphia, 1976).
[43] Y. V. Sharvin, Zh. Eksp. Teor. Fiz. **48**, 984 (1965).
[44] Y. V. Sharvin, Sov. Phys. JETP **21**, 655 (1965).
[45] E. P. Wigner, Phys. Rev. **40**, 749 (1932).
[46] R. Bertoncini and A. P. Jauho, Phys. Rev. B **44**, 3655 (1991).